

Lead-free piezoelectric ceramics based on $(1 - x)\text{BNKLLT} - x\text{BCTZ}$ binary solid solutions synthesized by the solid-state combustion technique

Chittakorn Kornphom^{1,2} · Naratip Vittayakorn³ · Theerachai Bongkarn^{1,2,4}

Received: 30 September 2015 / Accepted: 8 January 2016 / Published online: 19 January 2016
© Springer Science+Business Media New York 2016

Abstract The aim of this work is to improve the electrical properties of BNKLLT ceramics with the addition of BCTZ. New binary $(1 - x)\text{BNKLLT} - x\text{BCTZ}$ lead-free piezoelectric ceramics with different x contents between 0 and 0.10 (step 0.02) were fabricated by the solid-state combustion technique, where glycine was used as a fuel. The influences of x concentration on the phase evolution, morphology, and electrical behavior were investigated. The phase formation exhibited a coexistence of rhombohedral and tetragonal phases in all samples. With the increasing x content, the phase formation was dominated by a higher tetragonality. The average grain size continuously reduced from 1.52 to 0.96 μm when x content was increased. The maximum dielectric temperature (T_{SA}) of these ceramics decreased with the increasing x content. The ferroelectric properties were further weakened with the increasing x content. The MPB region was obtained at x content of around 0.04 producing this sample and showed the highest dielectric constants ($\epsilon_r = 2720$ and $\epsilon_{SA} = 6110$) and an excellent piezoelectric constant ($d_{33} = 295$ pC/N).

Introduction

Lead-based ceramics, for example, $\text{Pb}(\text{Mg}, \text{Nb})\text{O}_3$ -based, PbTiO_3 -based, and $\text{Pb}(\text{Zr}, \text{Ti})\text{O}_3$ -based ceramics are widely used in piezoelectric industry because of their excellent electrical properties and low cost. However, the toxicity of lead is a serious threat to human health and environment. Hence, lead-free ceramics with superior piezoelectric properties are required to replace the currently used toxic lead-based materials [1, 2]. The lead-free $(\text{Bi}_{0.5}\text{Na}_{0.5})\text{TiO}_3$ (BNT) is a key piezoelectric material which has received much attention since it has great potential to replace the lead-based piezoelectric materials. It shows high Curie temperature (320 °C) and large remnant polarization ($P_r = 38$ $\mu\text{C}/\text{cm}^2$) [3]. However, the applications of BNT ceramics in electronics have been limited by some weaknesses in BNT's electrical properties. These include a low dielectric constant ($\epsilon_r = 1000$), a low piezoelectric coefficient ($d_{33} = 90$ pC/N), a large coercive field ($E_c = 73$ kV/cm), and a high conductivity at room temperature [3]. Many researchers have attempted to improve the electrical properties of BNT ceramics by substituting some cations (K^+ and Li^+) [4, 5] on the A-site, by doping small amounts of cations (La^{3+} , Ga^{3+} , and Al^{3+}) [6–8] and including other compounds, for example: BaTiO_3 (BT) [9], KNaNbO_3 (KNN) [10], BiKTiO_3 (BKT) [11], and $(\text{Ba Ca})(\text{Zr Ti})\text{O}_3$ (BCTZ) [12] in the BNT ceramics.

The substitution of K^+ and Li^+ in the A-site of a BNT system at a composition of $\text{Bi}_{0.5}(\text{Na}_{0.68}\text{K}_{0.22}\text{Li}_{0.10})_{0.5}\text{TiO}_3$ (BNKLT) can improve the electrical properties of BNT by enhancing the d_{33} value (180 pC/N) and the dielectric constant (~ 1100) [5]. Moreover, the BNKLT system exhibits a low E_c value (~ 32 kV/cm), and the P_r value was about 31 $\mu\text{C}/\text{cm}^2$. Recently, Hong Pan et al. [13] modified the electrical properties of BNKLT by doping La_2O_3 . $\text{Bi}_{0.5}(\text{Na}_{0.68}\text{K}_{0.22}\text{Li}_{0.10})_{0.5}\text{TiO}_3$ with 0.10 wt% of La_2O_3

✉ Theerachai Bongkarn
researchcmu@yahoo.com

¹ Department of Physics, Faculty of Science, Naresuan University, Phitsanulok 65000, Thailand

² Research Center for Academic Excellence in Applied Physics, Faculty of Science, Naresuan University, Phitsanulok 65000, Thailand

³ Department of Chemistry, Faculty of Science, King Mongkut's Institute of Technology Ladkrabang, Ladkrabang, Bangkok 10520, Thailand

⁴ Research Center for Academic Excellence in Petroleum, Petrochemicals and Advanced Materials, Faculty of Science, Naresuan University, Phitsanulok 65000, Thailand

(abbreviated to BNKLLT) prepared by conventional solid-state method. This ceramic thus obtained exhibited a higher d_{33} value (192 pC/N) and a higher dielectric constant (~ 1254), and a lower E_c value (~ 29 kV/cm) compared with the BNKLLT ceramic. The P_r value of BNKLLT was about 29.4 which is close to that of the BNKLT system.

In the case of the binary system, Q. Gou's group [12] studied the solid solution of $0.94(\text{Bi}_{0.5}\text{Na}_{0.5}\text{TiO}_3) - 0.06(\text{Ba}_{0.85}\text{Ca}_{0.15})(\text{Ti}_{0.90}\text{Zr}_{0.10})\text{O}_3$ (abbreviated to BNT-BCTZ). This system showed d_{33} value (158 pC/N) and a dielectric constant (~ 1500) which were higher than those of pure BNT ceramics. Therefore, the substitution and doping of some cations combined with BCTZ in the right proportions are an effective way to enhance the piezoelectric properties of BNT ceramics. For this reason, the concept for fabrication of a new solid solution of BNKLLT combined with a BCZT concentration at composition in the range of 0–0.10 wt% to increase the piezoelectric, dielectric, and ferroelectric properties is of great interest and a challenge.

The conventional solid-state method requires a high firing temperature which leads to the evaporation of some raw materials, and the ceramics obtain a low density [13–15]. Recently, Bongkarn's works [15–19] successfully synthesized high-quality piezoelectric ceramics of a single system and a binary system by the solid-state combustion technique, for example: BNKLLT [15], BCTZ [16], BNKLT-BZT [17], BNT-BKT-BF [18], and BNLT-BZT [19]. This technique was modified from the solid-state reaction technique. The technical feature of the combustion technique is the released energy which is obtained from the decomposition reaction of the fuel that increases the rate of the chemical reaction of the raw materials. Moreover, the liquid phase resulting from the melting of the fuel creates a facile diffusion of the raw materials [20–22]. The powders obtained are of higher purity, are more homogenous, have a finer particle size, require lower firing temperature, and have a shorter dwell time than the powder synthesized via the conventional solid-state method [15–22].

From a review of the literature, it was found that the fabrication of new binary of $(1-x)\text{BNKLLT} - x\text{BCTZ}$ via the solid-state combustion technique had not been studied. In this work, the binary systems of $(1-x)\text{BNKLLT} - x\text{BCTZ}$ with $0 \leq x \leq 0.10$ were synthesized by the solid-state combustion technique. The effects of BCTZ contents on the phase formation, morphology, and electrical properties of $(1-x)\text{BNKLLT} - x\text{BCTZ}$ ceramics were methodically investigated.

Experimental

The solid-state combustion technique was used to fabricate $(1-x)(\text{Bi}_{0.5}(\text{Na}_{0.68}\text{K}_{0.22}\text{Li}_{0.1})_{0.5}\text{TiO}_3 + 0.10 \text{ wt}\% \text{ of } \text{La}_2\text{O}_3) - x(\text{Ba}_{0.90}\text{Ca}_{0.10})(\text{Ti}_{0.85}\text{Zr}_{0.15})\text{O}_3$ [$(1-x)\text{BNKLLT} -$

$x\text{BCTZ}$] ceramics at various contents of $x = 0, 0.02, 0.04, 0.06, 0.08, \text{ and } 0.10$, where glycine ($>98.5\%$, Ajax, NZ) was used as fuel. Highly pure reagents such as Bi_2O_3 ($>99\%$, Qręc, NZ), NaNO_3 ($>99\%$, Ajax, NZ), KHCO_3 ($>99\%$, Ajax, NZ), Li_2CO_3 ($>99\%$, Merck, DE), TiO_2 ($>99\%$, Ajax, NZ), La_2O_3 ($>99\%$, Aldrich, CN), BaCO_3 ($>99\%$, Ajax, NZ), $\text{Ca}(\text{NO}_3)_2 \cdot 4\text{H}_2\text{O}$ ($>99\%$ Ajax, NZ), and ZrO_2 ($>99\%$, Cerao, US) were used as raw materials. They were weighed by stoichiometric amounts and ball milled for 24 h in ethanol. Then, the suspensions were dried, and the obtained powders were sieved (500 mesh). The dried powders were mixed with glycine in a ratio of 1:0.56 for the $\text{Bi}_{0.5}(\text{Na}_{0.68}\text{K}_{0.22}\text{Li}_{0.1})_{0.5}\text{TiO}_3 + 0.1 \text{ wt}\% \text{ of } \text{La}_2\text{O}_3$ powder and a ratio of 1:1.11 for the $(\text{Ba}_{0.90}\text{Ca}_{0.10})(\text{Ti}_{0.85}\text{Zr}_{0.15})\text{O}_3$ powder [15, 16]. The BNKLLT and BCTZ powders were calcined at 750°C for 2 h and 1050°C for 2 h, respectively [15, 16]. Thereafter, the BNKLLT calcined powder and BCTZ calcined powder were mixed in various compositions and were milled with 3 wt% PVA aqueous in ethanol for 24 h. Then, the mixed calcined powders were pressed into pellets, 15 mm in diameter and 1.5 mm in thickness, under 80 MPa pressure. The green pellets were sintered at an optimum sintering temperature of 1100°C for $x = 0$ [15] and 1125°C for $0.02 \leq x \leq 0.10$ using a dwell time of 2 h [23] in air at a heating rate of $5^\circ\text{C}/\text{min}$ and allowed to cool down naturally. The sintered samples were coated with silver paste (Heraeus, D11402) on both sides and were fired at 500°C for 30 min. These were the electrodes for the electrical measurements. For piezoelectric testing, the samples were poled in a silicon oil bath under 3 kV/mm of dc field at 60°C for 30 min. The electric field was then decreased to zero kV/mm, and the samples were cooled down to room temperature. The phase formation and the morphologies of the samples were examined by X-ray diffraction (XRD, Philip PW 3040/60 X'Pert Pro) and scanning electron microscopy (SEM, Leo1455VP). The densities of the sintered samples were measured by the Archimedes method. The theoretical density values of these samples at various compositions were calculated according to the atomic weight and unit cell lattice parameters from the XRD data [2]. The average grain size of the sintered ceramics was determined by means of the linear interception method on SEM images of polished samples which had been thermally etched for 10 min at a temperature 100°C below the sintering temperature [2]. The raw data were obtained by measuring the grain sizes over 300 grains. Dielectric properties were measured using a LCR meter (HP, 4284A) at a frequency of 1 kHz. The properties were measured over the temperature range of $25\text{--}400^\circ\text{C}$ at a heating rate of $1^\circ\text{C}/\text{min}$, which was controlled using an Eurotherm system (2408 CP) with the raw data of dielectric properties being collected every 4 s. The piezoelectric constant d_{33} values were measured using a quasi-static d_{33} -meter (Sinocera,

YE2730A). The ferroelectric properties were determined at room temperature using a computer-controlled, modified Sawyer–Tower circuit (Radiant, PLC2-1014346).

Results and discussion

Figure 1a exhibits the XRD patterns obtained from the $(1-x)\text{BNKLLT}-x\text{BCTZ}$ samples in the 2θ range of 10° – 60° as a function of x content. A pure perovskite phase was observed in all samples and no impurity phase was observed in the range of detection. This indicated that a stable solid solution was formed between the BNKLLT and BCTZ. To better understanding the effect of BCTZ content on $(1-x)\text{BNKLLT}-x\text{BCTZ}$ phase structure, the expanded XRD patterns with 2θ around 40° and 46° are presented in Fig. 1b and c. As for the rhombohedral structure, it was characterized by dual $(003)/(021)_R$ peaks at around 40° and a single $(202)_R$ peak at around 46° [6, 12, 15]. An analysis of the tetragonal structure demonstrated a single peak of $(111)_T$ and dual peaks of $(002)/(200)_T$ at around 40° and 46° , respectively [15]. At x content of 0, the peak position at 40° showed an unclear splitting of $(003)/(021)_R$ dual peaks (Fig. 1b) and no symmetry of a single $(202)_R$ peak was observed at 46° (Fig. 1c) which indicated the coexistence of both rhombohedral and tetragonal phases. This result was similar to BNKLLT ceramics prepared by combustion technique [15]. When the x content was increased, the dual peaks position of $(003)/(021)_R$ began to fuse into a single peak of $(111)_T$ (Fig. 1b) while a single

peak position of $(202)_R$ evidently split into the dual $(002)/(200)_T$ peaks (Fig. 1c), which assumed that the tetragonality of the ceramics was increased. Moreover, the peak positions at around 40° and 46° gradually shifted to a low angle with increasing BCTZ content which suggests that the unit cell volume enlarged. The enlargement of unit cell volume was caused by some replacement of $\text{Ba}^{2+}/\text{Ca}^{2+}$ for $(\text{Bi}/\text{Na})^{2+}$ at A-site and Zr^{4+} for Ti^{4+} at B-sites. The ionic radius of the dominated Ba^{2+} ($r_{\text{Ba}^{2+}} = 1.61 \text{ \AA}$) at the A-site and Zr^{4+} ($r_{\text{Zr}^{4+}} = 0.72 \text{ \AA}$) at the B-site are larger than the radii of the $(\text{Bi}/\text{Na})^{2+}$ ($r_{\text{Bi}^{3+}} = 1.40 \text{ \AA}$ and $r_{\text{Na}^+} = 1.39 \text{ \AA}$) at the A-sites and Ti^{4+} ($r_{\text{Ti}^{4+}} = 0.605 \text{ \AA}$) at the B-site [10].

Typical SEM morphology images of $(1-x)\text{BNKLLT}-x\text{BCTZ}$ ceramics with different x contents are shown in Fig. 2a–f. The grain morphologies of all samples showed irregular grain shape (Fig. 2a–f). At x content of 0, the small porosity was observed, and there is relatively uniform grain size (Fig. 2a). At x content between 0.02 and 0.10, the porosity increased obviously, and the size of grain exhibited to be more intermittent when x content increased (Fig. 2b–f). The average grain size of the $(1-x)\text{BNKLLT}-x\text{BCTZ}$ ceramics decreased from 1.52 to $0.96 \mu\text{m}$ when x concentration increased from 0 to 0.10 and is exhibited in Fig. 3. The decrease of the grain size was caused by the reduction of mobility of the grain boundary, which resulted in the grain growth being inhibited [12]. The resulting densities of the $(1-x)\text{BNKLLT}-x\text{BCTZ}$ ceramics with various x contents are also displayed in Fig. 3. The density values of these ceramics gradually

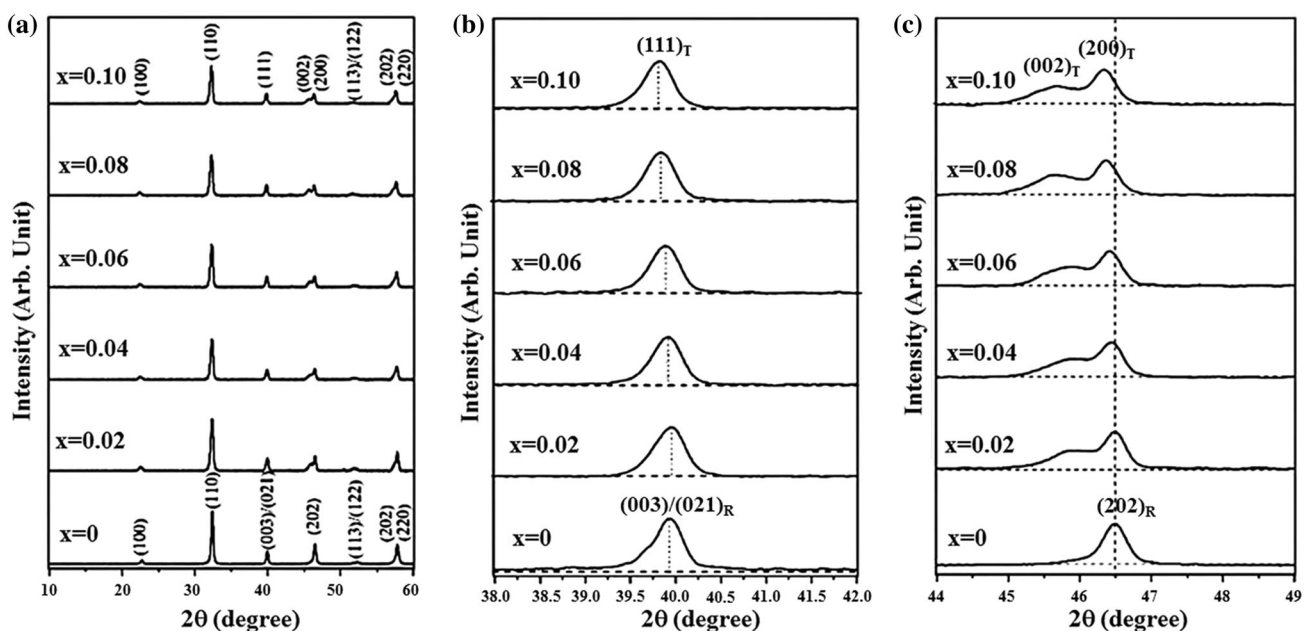


Fig. 1 a XRD patterns and expanded XRD patterns with 2θ ranging from **b** 38° – 42° and **c** 44° – 49° of $(1-x)\text{BNKLLT}-x\text{BCTZ}$ samples as a function of x content

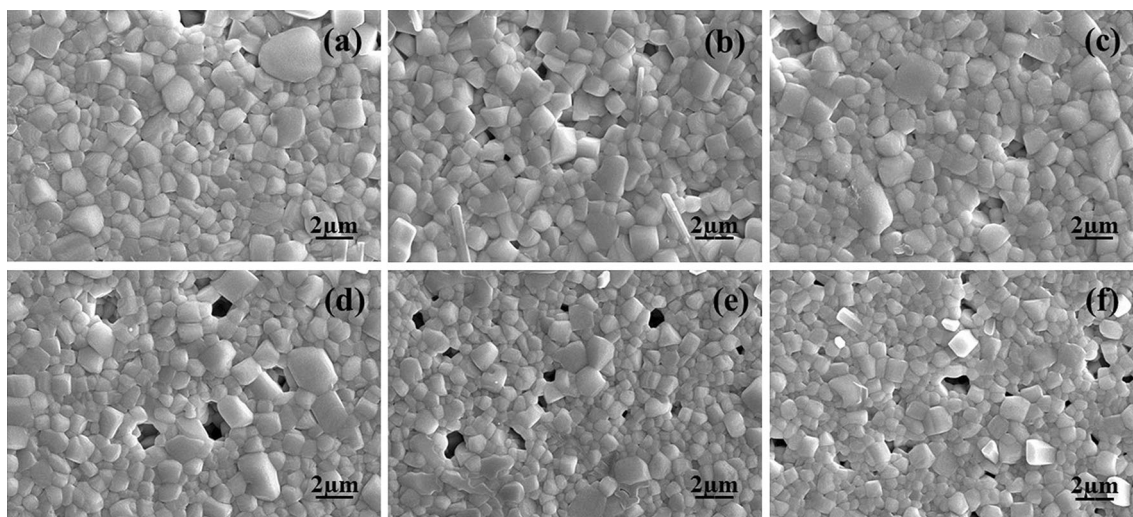


Fig. 2 SEM surface morphologies of $(1 - x)\text{BNKLLT}-x\text{BCTZ}$ ceramics with various x contents. **a** $x = 0$, **b** $x = 0.02$, **c** $x = 0.04$, **d** $x = 0.06$, **e** $x = 0.08$, and **f** $x = 0.10$

decreased from 5.76 to 5.63 g/cm^3 when the BCTZ content was increased, and the theoretical density values are listed in Table 1. The theoretical density of the $(1 - x)\text{BNKLLT}-x\text{BCTZ}$ ceramics corresponded with the microstructure’s result.

Dielectric constant (ϵ) and dielectric loss ($\tan\delta$) values measured at frequencies between 1 and 100 kHz of $(1 - x)\text{BNKLLT}-x\text{BCTZ}$ ceramic with x content of 0.04 plotted as a function of unpoled and poled sample are shown in Fig. 4. At the unpoled sample (Fig. 4a), the dielectric constant (ϵ) includes two anomaly peaks of broad dielectric curve: the first anomaly of a frequency dispersion appearing at a lower temperature (It will be identified by a subscript “FA”) and the second anomaly appearing at higher temperature (It will be identified by a subscript

“SA”). The peak of dielectric loss at a lower temperature ($\tan \delta_{\text{FA}}$) demonstrated a broad peak shape and a strong frequency dispersion. The temperature for $\tan \delta_{\text{FA}}$ was lower than that in the dielectric constant (ϵ_{FA}). At higher temperature, the dielectric loss peak ($\tan \delta_{\text{SA}}$) showed a frequency dispersion, and the magnitudes of the peak value decrease when frequency increased. These results were similar to the dielectric results of BNT—6 mol% BT and BNT—BKT modified with BZT in the previous works as reported by Jo et al. [24] and Dittmer et al. [25], respectively. They assumed that the anomalies of dielectric curve relate with a thermal evolution of relaxation time distribution or correlation length distribution of the polar nanoregions (PNRs), which has nothing to do with any measurable phase transition [24, 25]. The dielectric constants and losses of poled $(1 - x)\text{BNKLLT}-x\text{BCTZ}$ samples are demonstrated in Fig. 4b. A discontinuous change in dielectric constant and loss was observed at $\sim 87^\circ\text{C}$ which corresponded to the temperature where the electric-field-induced ferroelectric order transformed back to relaxer [24, 25].

Figure 5 presents the dielectric behaviors of the $(1 - x)\text{BNKLLT}-x\text{BCTZ}$ binary system with $0 \leq x \leq 0.10$, which were measured at a frequency of 1 kHz. For all compositions of x content, the dielectric response demonstrated two anomaly peaks of ϵ_{FA} and ϵ_{SA} near $134\text{--}139^\circ\text{C}$ (T_{FA}) and $321\text{--}338^\circ\text{C}$ (T_{SA}), respectively, in all compositions. The dielectric peak at T_{FA} demonstrated increased broadness with the increasing x content. The T_{FA} gradually increased when the x content was increased up to 0.04, and then decreased as listed in Table 1. The T_{SA} tended to reduce from 338 to 321 $^\circ\text{C}$ when the x content increased from 0 to 0.10 (Table 1). Similar to the results of

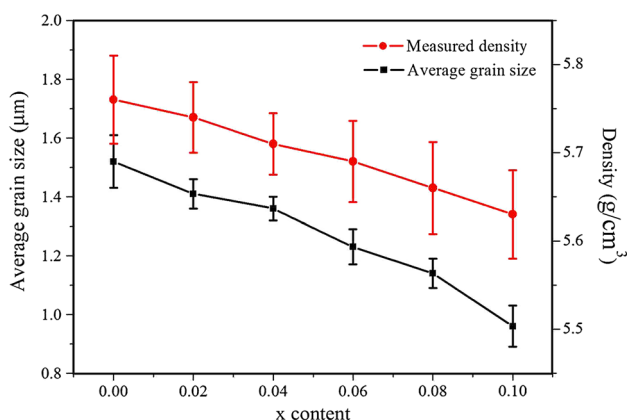
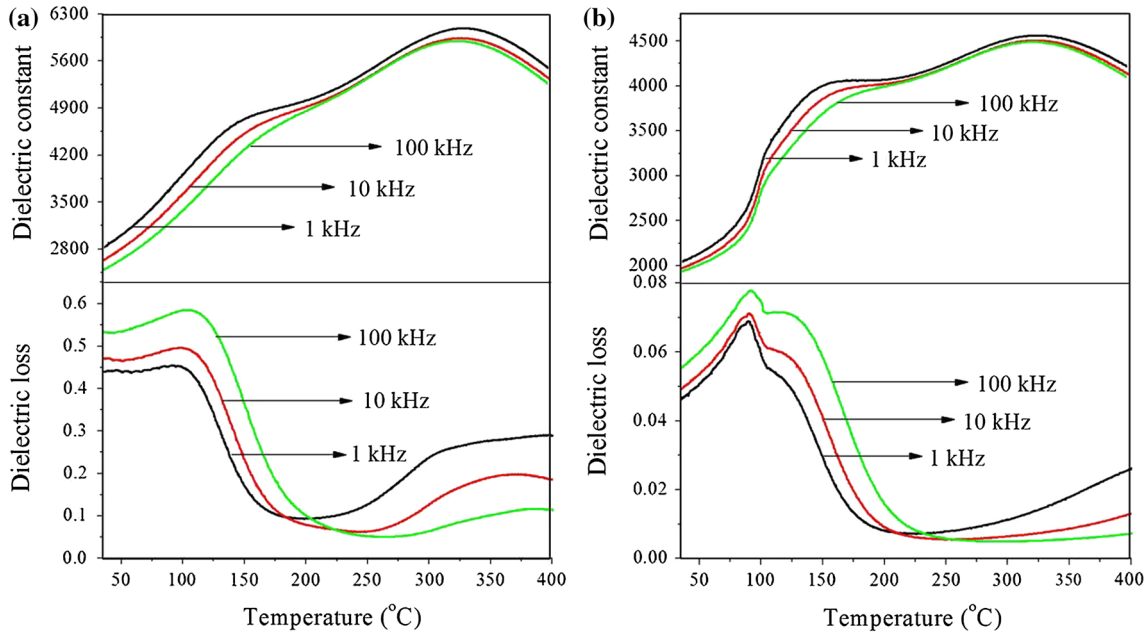
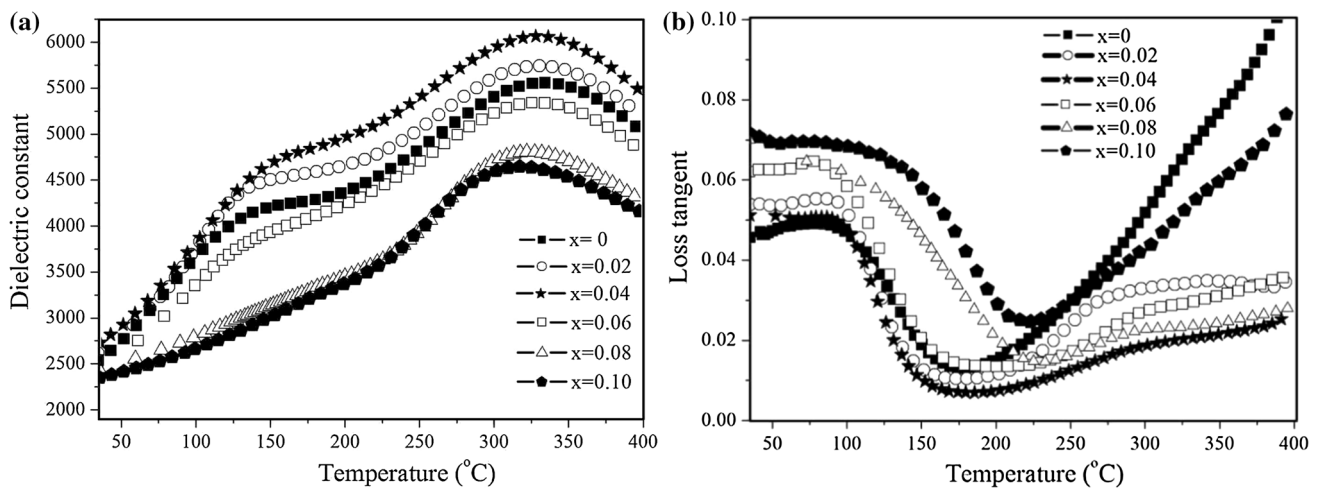


Fig. 3 Average grain sizes and measured densities of $(1 - x)\text{BNKLLT}-x\text{BCTZ}$ ceramics with different x contents

Table 1 Theoretical densities, T_{FA} , T_{SA} , dielectric properties, ferroelectric properties, and d_{33} of $(1-x)\text{BNKLLT}-x\text{BCTZ}$ ceramics

x	Theoretical density (%)	ϵ_r	$\tan\delta$ at T_r	ϵ_{SA}	$\tan\delta$ at T_{SA}	T_{FA} ($^{\circ}\text{C}$)	T_{SA} ($^{\circ}\text{C}$)	P_r ($\mu\text{C}/\text{cm}^2$)	E_c (kV/cm)	d_{33} (pC/N)
0	96.7 ± 0.84	2572	0.042	5536	0.071	134	338	35.8	22.42	210
0.02	96.4 ± 0.67	2629	0.055	5734	0.034	135	334	31.2	19.35	267
0.04	96.1 ± 0.59	2720	0.052	6110	0.022	139	329	29.8	18.21	295
0.06	95.8 ± 0.77	2494	0.063	5278	0.029	137	326	24.5	15.45	227
0.08	95.6 ± 0.88	2421	0.070	4775	0.025	134	324	20.1	12.78	188
0.10	95.3 ± 0.85	2372	0.072	4621	0.055	130	321	13.6	10.72	155

**Fig. 4** Temperature dependences of dielectric properties of $(1-x)\text{BNKLLT}-x\text{BCTZ}$ ceramics at a content of $x = 0.04$ measured at frequencies in the range of 1–100 kHz. **a** unpoled and **b** poled samples**Fig. 5** Temperature dependences of **a** dielectric constant and **b** dielectric loss of the $(1-x)\text{BNKLLT}-x\text{BCTZ}$ ceramics at different of x content and measured at a frequency of 1 kHz

previous works of BNT–BT and BNT–BCZT [9, 12], the increment and following reduction of T_{FA} were a result of the oxygen octahedron which may have been twisted, and the subsequent reduction of T_{FA} was caused by the BCTZ content exhibiting a low Curie temperature [10]. The dielectric constant at room temperature (ϵ_r) and maximum dielectric constant (ϵ_{SA}) increased from 2572 to 2720 and 5536 to 6110, respectively, when the BCTZ content was increased up to 0.04, and then decreased with a further increase in BCTZ content (Table 1). The dielectric losses ($\tan\delta$) at room temperature (T_r) and at T_{SA} of $(1-x)\text{BNKLLT}-x\text{BCTZ}$ are listed in Table 1. The highest values of 2720 and 6110 were recorded by the samples at a composition of $x = 0.04$. The ϵ_r value of $(1-x)\text{BNKLLT}-x\text{BCTZ}$ at x content of 0.04 was much higher than those of both the pure BNKLLT ceramic and the binary system of BNT–BCTZ. When pure BNKLLT was prepared by the solid-state reaction technique and the combustion technique, ϵ_r values were about ~ 1500 , and ~ 2500 pC/N, respectively [13, 15]. In case of BNT–BCTZ binary ceramics, it was about ~ 1200 [12].

The polarization versus the electric field hysteresis loops (P – E) at room temperature of $(1-x)\text{BNKLLT}-x\text{BCTZ}$ ceramics as a function of x concentration measured by electric field of 30 kV/cm are shown in Fig. 6a–f. The ferroelectric behavior of the $(1-x)\text{BNKLLT}-x\text{BCTZ}$ ceramics was significantly affected with the addition of x content. It was observed that the ceramics with x content of 0 exhibited unsaturated P – E loops (Fig. 6a) which was

similar to results found in previous works [13, 15]. At an x concentration between 0.02 and 0.04, these P – E loops became more saturated with the increasing x content (Fig. 6b, c). When the x content increased from 0.06 to 0.08, the P – E loops were more saturated (Fig. 6d, e), which assumed that the polarization was more easily switched at the same induced electric field when the BNKLLT was combined with the BCTZ [26–28]. However, when the x concentration was further increased to 0.10, the P – E loops displayed were not fully saturated and were further slanted (Fig. 6f), indicating the weakening of its ferroelectric properties. The remnant polarization (P_r) and the coercive field (E_c) values of $(1-x)\text{BNKLLT}-x\text{BCTZ}$ decreased successively when the x concentration was increased, and are listed in Table 1. In previous work, it was observed that the ferroelectric behavior of the BNT-based ceramics correlate with the grain size [29]. The coupling between grain boundaries and domain walls becomes very strong when grain size is nearly or less than that of 1 μm [29, 30]. The stronger coupling made the ferroelectric properties become weaker because of the decrease in the domain wall mobility and domain alignment. In this work, the $(1-x)\text{BNKLLT}-x\text{BCTZ}$ ceramics displayed the smaller grain the with the increasing x content which led to the weak ferroelectric properties.

The measurement of the piezoelectric coefficients (d_{33}) in $(1-x)\text{BNKLLT}-x\text{BCTZ}$ system as a function of x concentration is listed in Table 1. The d_{33} values increased from 210 pC/N to 295 pC/N with the increasing

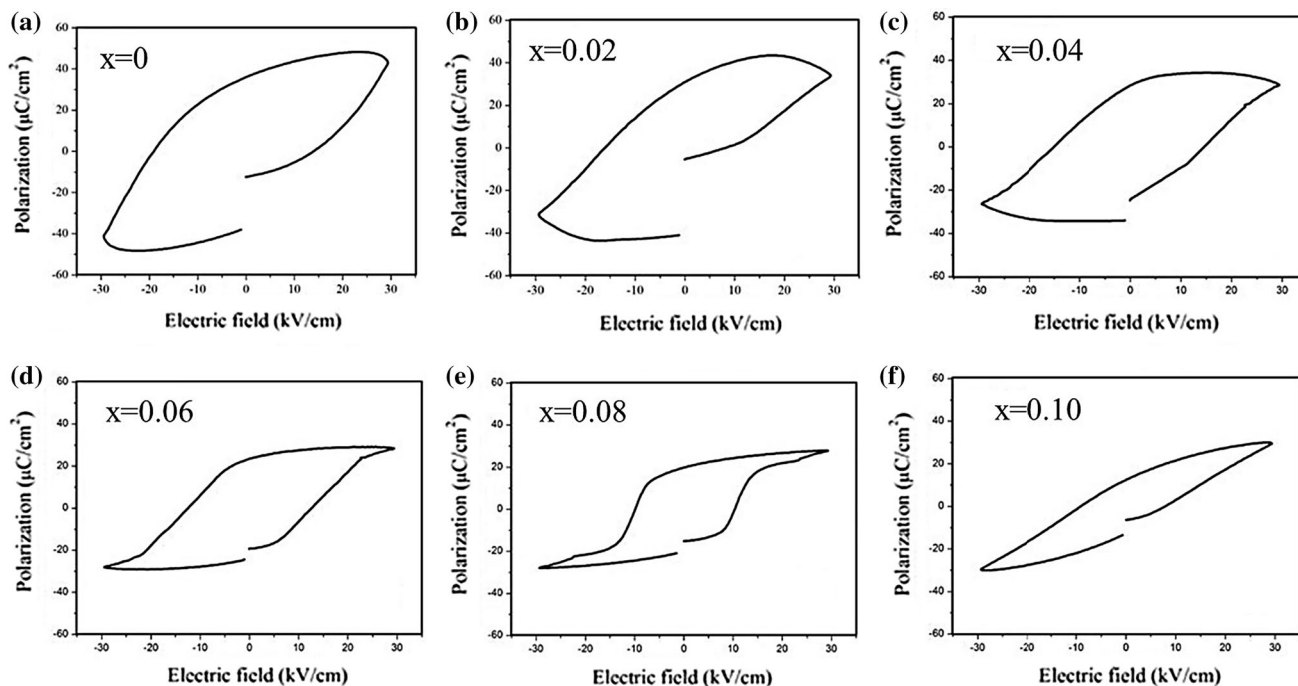


Fig. 6 P – E loops of $(1-x)\text{BNKLLT}-x\text{BCTZ}$ ceramics as a function of x content, measured at 30 kV/cm and room temperature

x content from 0 to 0.04. Then, the d_{33} values decreased in turn with a further increase of BCTZ contents >0.04 . The x content of 0.04 attained a maximum value of 295 pC/N which was much higher than those of both the pure BNKLLT ceramic and the binary system of BNT–BCTZ. When pure BNKLLT was prepared by the solid-state reaction method and combustion technique, d_{33} values were about ~ 192 and ~ 210 pC/N, respectively [13, 15]. In case of BNT–BCTZ binary ceramics, it was about ~ 158 pC/N [12]. It is well known that the high piezoelectric constants (d_{33}) can be obtained from the coexistence phase because the direction of polarization is easily rotated by external stress or the electric field, which result from the instability of the polarization state [27]. Hence, a $(1-x)$ BNKLLT– x BCTZ sample at an x content of 0.04 defines a morphotropic phase boundary (MPB) because the phase formation displayed coexistence structure of the rhombohedral and tetragonal structures which exhibit an excellent dielectric constant and a large piezoelectricity. The introduction of a suitable amounts of BCTZ in BNKLLT ceramics is one of the choices to optimize the piezoelectric behavior of the lead-free ceramics.

Conclusion

A novel binary $(1-x)$ BNKLLT– x BCTZ lead-free piezoelectric solid solution as a function of x contents was synthesized by the solid-state combustion technique using glycine as a fuel. All samples expressed the coexistence phase between rhombohedral and tetragonal. The tetragonality increased with the increasing x concentration. The decrease of average grain size, T_{SA} and the weak ferroelectricity of these ceramics with the increasing x content were observed. The MPB region was obtained by the sample at a composition of $x = 0.04$, which exhibited the highest dielectric constant ($\epsilon_r = 2720$ and $\epsilon_{SA} = 6110$) and excellent d_{33} (295 pC/N). This paper provides a new way to modify dielectric and piezoelectric behaviors of BNT lead-free materials.

Acknowledgements This work was supported by the Higher Education Research Promotion and National Research University project of Thailand, Office of the Higher Education Commission. The authors wish to thank the Department of Physics, Faculty of Science, Naresuan University for the supporting facilities. Thanks are also due to Mr. Don Hindle for his help in editing the manuscript.

References

- Rodel J, Jo W, Seifert KTP, Anton EM, Granzow T (2009) Perspective on the development of lead-free piezoceramics. *J Am Ceram Soc* 92:1153–1177
- Bai Y, Matousek A, Tofel P, Bijalwan V, Nan B, Hughes H, Button TW (2015) (Ba, Ca)(Zr, Ti)O₃ lead-free piezoelectric ceramics—the critical role of processing on properties. *J Eur Ceram Soc* 35:3445–3456
- Smolenskii GA, Isupov VA, Agranovskaya AI, Krainik NN (1961) New ferroelectrics of complex composition. *Phys Solid State* 2(11):2651–2654
- Li YM, Chen W, Zhou J, Xu Q, Sun HJ, Liao MS (2005) Dielectric and ferroelectric properties of lead-free Na_{0.5}Bi_{0.5}TiO₃–K_{0.5}Bi_{0.5}TiO₃ ferroelectric ceramics. *Ceram Int* 31(1):139–142
- Yang ZP, Hou YT, Pan H, Chang YF (2009) Structure, microstructure and electrical properties of $(1-x-y)$ Bi_{0.5}Na_{0.5}TiO₃– x Bi_{0.5}K_{0.5}TiO₃– y Bi_{0.5}Li_{0.5}TiO₃ lead-free piezoelectric ceramics. *J Alloys Compd* 480:246–253
- Herabut A, Safari AM (1997) Processing and electromechanical properties of (Bi_{0.5}Na_{0.5})_(1-1.5x)La_xTiO₃ ceramics. *J Am Ceram Soc* 80:2954–2958
- Zhou CR, Liu XY, Li WZ, Yuan CL, Chen GH (2010) Structure and electrical properties of Bi_{0.5}(Na, K)_{0.5}TiO₃–BiGaO₃ lead-free piezoelectric ceramics. *Curr Appl Phys* 10:93–98
- Baettig P, Schelle CLF, LeSar RC, Waghmare UV, Spaldin NCA (2005) Theoretical prediction of new high-performance lead-free piezoelectrics. *Chem Mater* 17:1376–1380
- Takenaka T, Maruyama KI, Sakata K (1991) (Bi_{1/2}Na_{1/2})TiO₃–BaTiO₃ system for lead-free piezoelectric ceramics. *Jpn J Appl Phys* 30:2236–2239
- Kounga AB, Zhang ST, Jo W, Granzow TT, Rödel JG (2008) Morphotropic phase boundary in lead-free piezoceramics. *Appl Phys Lett* 92:222902
- Ji WJ, Chen YB, Zhang ST, Yang B, Zhao XN, Wang QJ (2012) Microstructure and electric properties of lead-free 0.8Bi_{1/2}Na_{1/2}TiO₃–0.2Bi_{1/2}K_{1/2}TiO₃ ceramics. *Ceram Int* 38:1683–1686
- Gou Q, Wu JG, Li AG, Wu B, Xiao DG, Zhu JG (2012) Enhanced d_{33} value of Bi_{0.5}Na_{0.5}TiO₃–(Ba_{0.85}Ca_{0.15})(Ti_{0.90}Zr_{0.10})O₃ lead-free ceramics. *J Alloys Compd* 521:4–7
- Pan H, Hou YT, Chao XL, Wei LL, Yang ZP (2011) Microstructure and electrical properties of La₂O₃-doped Bi_{0.5}(Na_{0.68}K_{0.22}Li_{0.1})_{0.5}TiO₃ lead-free piezoelectric ceramics. *Curr Appl Phys* 11:888–892
- Naderer MC, Schütz DN, Kainz TR, Reichmann K, Mittermayr FR (2012) The formation of secondary phases in Bi_{0.5}Na_{0.375}K_{0.125}TiO₃ ceramics. *J Euro Ceram Soc* 32:2399–2404
- Bhupajit P, Kornphom C, Vittayakorn N, Bongkarn T (2015) Structural, microstructure and electrical properties of La₂O₃-doped Bi_{0.5}(Na_{0.68}K_{0.22}Li_{0.1})_{0.5}TiO₃ lead-free piezoelectric ceramics synthesized by the combustion technique. *Ceram Int* 41:81–86
- Kornphom C, Vittayakorn N, Bongkarn T (2016) Low firing temperatures and high ferroelectric properties of (Ba_{0.85}Ca_{0.15})(Ti_{0.90}Zr_{0.10})O₃ lead-free ceramics synthesized by the combustion technique. *Ferroelectric*. doi:10.1080/00150193.2015.1070239
- Kornphom C, Laowanidwatana A, Bongkarn T (2013) The effects of sintering temperature and content of x on phase formation, microstructure and dielectric properties of $(1-x)$ (Bi_{0.4871}Na_{0.4871}La_{0.0172}TiO₃)– x (BaZr_{0.05}Ti_{0.95}O₃) ceramics prepared via the combustion technique. *Ceram Int* 39:421–426
- Sumang R, Vittayakorn N, Bongkarn T (2013) Crystal structure, microstructure and electrical properties of $(1-x-y)$ Bi_{0.5}Na_{0.5}TiO₃– x Bi_{0.5}K_{0.5}TiO₃– y BiFeO₃ ceramics near MPB prepared via the combustion technique. *Ceram Int* 39:409–413
- Julphunthong P, Bongkarn T (2014) Phase formation, microstructure and dielectric properties of Bi_{0.5}(Na_{0.74}K_{0.16}Li_{0.10})_{0.5}TiO₃–Ba(Zr_{0.5}Ti_{0.95})O₃ ceramics prepared via combustion technique. *Mater Res Innov* 18(S2):151–156

20. Wattanawikkam C, Vittayakorn N, Bongkarn T (2013) Low temperature fabrication of lead-free KNN-LS-BS ceramics via the combustion method. *Ceram Int* 39:399–403
21. Razak K, Yip CJ, Sreekantan S (2011) Synthesis of $(\text{Bi}_{0.5}\text{Na}_{0.5})\text{TiO}_3$ (BNT) and Pr doped BNT using the soft combustion technique and its properties. *J Alloys Compd* 509:2936–2941
22. Manoharan SS, Patil KC (1992) Combustion synthesis of metal chromite powders. *J Am Ceram Soc* 75:1012–1015
23. Kornphom C, Combustion technique synthesis and characterization of new BNKLLT-BCTZ-NKLNST system ceramics. PhD Dissertation. Naresuan University, Thailand (In progress)
24. Jo W, Schaab S, Sapper EA, Schmitt L, Kleebe HJ, Bell AJ, Rödel J (2011) On the phase identity and its thermal evolution of lead free $(\text{Bi}_{1/2}\text{Na}_{1/2})\text{TiO}_3$ -6 mol% BaTiO_3 . *J Appl Phys* 110:074106
25. Dittmer R, Jo W, Daniels J, Schaab S, Rödel J (2011) Relaxor characteristics of morphotropic phase boundary $(\text{Bi}_{1/2}\text{Na}_{1/2})\text{TiO}_3$ - $(\text{Bi}_{1/2}\text{K}_{1/2})\text{TiO}_3$ modified with $\text{Bi}(\text{Zn}_{1/2}\text{Ti}_{1/2})\text{O}_3$. *J Am Ceram Soc* 94:4283–4290
26. Tian HY, Wang DY, Lin DM, Zeng JT, Kwok KW, Chan HLW (2007) Diffusion phase transition and dielectric characteristics of $\text{Bi}_0.5\text{Na}_0.5\text{TiO}_3$ - $\text{Ba}(\text{Hf}, \text{Ti})\text{O}_3$ lead-free ceramics. *Solid State Commun* 142:10–14
27. Chen XY, Wu JG, Cheng XJ, Wu B, Wu WJ, Xiao DQ, Zhu JG (2012) Piezoelectric properties of $[\text{Li}_{0.03}(\text{K}_{0.48}\text{Na}_{0.52})_{0.97}](\text{Nb}_{0.97}\text{Sb}_{0.03})\text{O}_3$ - $(\text{Ba}_{0.85}\text{Ca}_{0.15})(\text{Ti}_{0.90}\text{Zr}_{0.10})\text{O}_3$ lead-free piezoelectric ceramics. *Curr Appl Phys* 12:752–754
28. Xu Q, Chen M, Chen W, Liu HX, Kim BH, Ahn BK (2008) Effect of CoO additive on structure and electrical properties of $(\text{Na}_{0.5}\text{Bi}_{0.5})_{0.93}\text{Ba}_{0.07}\text{TiO}_3$ ceramics prepared by the citrate method. *Acta Mater* 56:642–650
29. Buessem WR, Cross LE, Goswami AK (1966) Phenomenological theory of high permittivity in fine-grained barium titanate. *J Am Ceram Soc* 49:33–36
30. Zhao XM, Chen XM, Wang J, Liang XX, Zhou JP, Liu P (2015) Effects of Ti nonstoichiometry on microstructure, dielectric, ferroelectric and piezoelectric properties of $(\text{Na}_{0.5}\text{Bi}_{0.5})_{0.94}\text{Ba}_{0.06}\text{Ti}_{1+x}\text{O}_3$ lead-free ceramics. *J Ceram Process Res* 16:18–23